Probing superconducting anisotropy of single crystal $KCa_2Fe_4As_4F_2$ by magnetic torque measurements

A. B. Yu,[1,3,4] T. Wang,[1,3] Y. F. Wu,[1,3,4] Z. Huang,[1,3] H. Xiao,[2] G. Mu,[1,3] and T. Hu[1,3,*]

[1]*State Key Laboratory of Functional Materials for Informatics, Shanghai Institute of Microsystem and Information Technology, Chinese Academy of Sciences, Shanghai 200050,China*

[2]*Center for High Pressure Science and Technology Advanced Research, Beijing 100094, China*

[3]*CAS Center for Excellence in Superconducting Electronics (CENSE), Shanghai 200050, China*

[4]*University of Chinese Academy of Science, Beijing 100049, China*

(Received 11 September 2019; published 14 October 2019)

Anisotropy is the key to understanding iron-based superconductors, which usually have quasi-two-dimensional layered structures. By using torque measurements (a sensitive tool to detect the magnetic anisotropy), we investigate the superconducting anisotropy of the $KCa_2Fe_4As_4F_2$ (12442, $T_c = 33$ K) single crystal. In the normal state, the torque data display a paramagnetic behavior $H^2 \sin 2\theta$ in different applied magnetic fields H aligned at an angle θ to the c axis of the crystal, while in the mixed state vortex torque dominates the torque signal. The anisotropy parameter γ and London penetration depth λ were obtained from vortex torque analyzed using Kogan's formula. It was found that γ is 16.2 at $T = 25$ K ($\approx 0.76\ T_c$), close to $\gamma \approx 15$ at $T \approx 0.76\ T_c$ for $CaFe_{0.88}Co_{0.12}AsF$, but much larger than the result of 11 and 122 families, where γ is around 3. In addition, the obtained perpetration depth from the torque measurements is consistent with the results of μSR measurements of $KCa_2Fe_4As_4F_2$. Our results suggest that the two-dimensionality plays a vital role in the superconductivity of the 12442-type iron-based superconductor.

DOI: 10.1103/PhysRevB.100.144505

I. INTRODUCTION

The recently discovered 12442-type iron-based superconductors (FeSCs) $AB_2Fe_4As_4C_2$ (A = K, Rb, Cs; B = Ca, Nd, Sm, Gd, Tb, Dy, Ho; C = F, O) [1–5] where $T_c = 28$–37 K have attracted a lot of interest. The 12442 system has a superstructure composed of 1111-type and 122-type FeSCs resembling the cuprate superconductors with double CuO_2 sheets [6]. This family exhibits an intrinsic hole conduction superconductivity and a dome-shaped superconducting phase [7], suggesting unconventional superconductivity [8]. Previous investigations showed the 12442 family has a significantly large anisotropy in both the normal and the superconducting state [6]. This kind of strongly anisotropic behavior is reminiscent of those of most cuprate superconductors, which makes the 12442 family different from the commonly known FeSCs with relatively small anisotropy [9]. First-principles studies suggest that the special crystal structure yields the two-dimensional electronic structure with six hole-type cylindrical Fermi-surface sheets and four electron-type ones, and consequently the large anisotropy [8,10,11].

In an anisotropic magnetic system, the vector quantities, like applied magnetic field $\vec{H}$ and magnetization $\vec{m}$, are no longer collinear unless they lie along the principal axis. Thus the magnetic torque $\vec{\tau} = \vec{m} \times \vec{H}$ is sensitive to the magnetic anisotropy. According to the anisotropic Ginzburg-Landau (GL) theory, the superconducting anisotropy parameter γ can be determined by the vortex torque, where $\gamma \equiv \sqrt{m_c^*/m_a^*} = H_{c2}^{\|c}/H_{c2}^{\|a} = \lambda_c/\lambda_a = \xi_a/\xi_c$ where a and c are directions along the crystal axes, m^* is the effective mass, H_{c2} is the upper critical field, λ is the penetration depth, and ξ is the coherence length [12]. Kogan's model derived from the anisotropic GL theory was wildly applied to study vortex torque. By analyzing vortex torque with Kogan's formula [13], one can obtain not only the γ but also the superconducting London penetration depth λ that can identify the ability of a superconductor to screen an applied field by the diamagnetic response of the superconducting condensate [14].

In this paper, detailed angular dependent torque measurements were performed on $KCa_2Fe_4As_4F_2$ single crystal in both normal and superconducting states. A large paramagnetic torque signal is observed in the normal state, while vortex torque is found at temperatures below T_c. The temperature and magnetic field dependent anisotropy parameter γ and the in-plane penetration depth λ_{ab} are obtained by fitting the reversible torque curves $\tau_{rev}(\theta)$ in the mixed state with the Kogan model. It is found that $KCa_2Fe_4As_4F_2$ has almost the same anisotropy as the 1111 families but is more anisotropic than 11 and 122 families. In addition, the obtained superconductor penetration depth λ_{ab} from torque measurements agrees with μSR measurements.

II. EXPERIMENT

A high-quality single crystal of $KCa_2Fe_4As_4F_2$ was grown using the self-flux method with KAs as the flux. The details on sample growth and other information can be found elsewhere [6]. Magnetization measurements were performed by

*thu@mail.sim.ac.cn

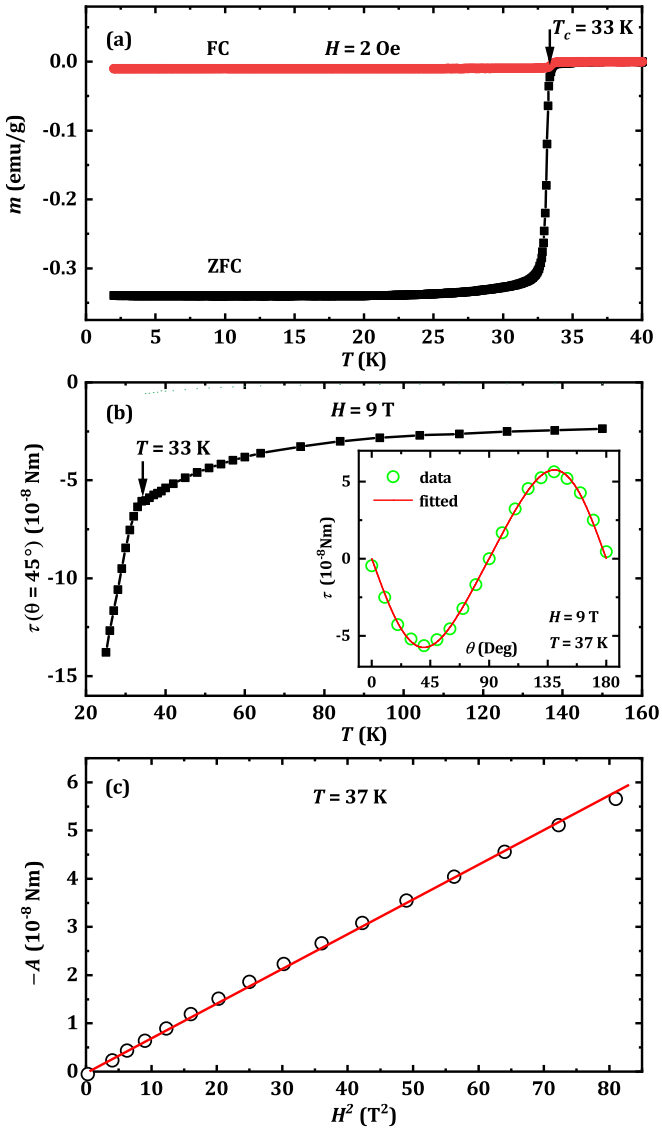

FIG. 1. (a) Single-crystal $KCa_2Fe_4As_4F_2$'s magnetization data at $H = 2$ Oe under field cooled (FC) and zero-field cooled (ZFC) conditions. (b) The $\tau(\theta = 45^\circ)$ dependent temperature above and below T_c for $H = 9$ T. Inset: Angular θ dependent torque τ data (open circle) measured at temperature $T = 37$ K with a magnetic field $H = 9$ T and fitting result (red line) by $A \sin 2\theta$. (c) A vs H^2 at $T = 37$ K.

using the Quantum Design superconducting quantum interference device. The angular (θ) dependent torque measurements were carried out using a piezoresistive torque magnetometer in the physical property measurement system. We define the angle between the c axis of the sample and magnetic field as θ. The increasing angle torque (τ_{inc}) and the decreasing angle torque (τ_{dec}) were measured at a temperature range of $25 \leqslant T \leqslant 150$ K and the applied magnetic field range $0.5 \leqslant H \leqslant 9$ T.

III. DISCUSSION

Figure 1(a) shows the temperature (T) dependent field cooled (FC) and zero-field cooled (ZFC) magnetization (m) curves measured at magnetic field H of 2 Oe applied along the c axis of the crystal. It is shown that the ZFC magnetization (m_{ZFC}) decreases suddenly at 33 K while the FC susceptibility (m_{FC}) keeps constant as it cools down. The decrease of m_{ZFC} at 33 K is due to the presence of a superconducting transition of $KCa_2Fe_4As_4F_2$ and the constant m_{FC} suggests a strong vortex pinning effect as observed usually in iron-based superconductors [15].

The inset to Fig. 1(b) shows the typical angular θ dependent torque $\tau(\theta)$ curves in the normal state. It is found that $\tau(\theta)$ (the green solid) is fitted well with the equation of $A \sin 2\theta$ (the red curve). Thus the torque measured at 45° [$\tau(\theta = 45^\circ)$] represents A, the amplitude of torque in the normal state. The main plot of Fig. 1(b) shows the temperature-dependent $\tau(\theta = 45^\circ)$ measured above and below $T_c = 33$ K and at the magnetic field $H = 9$ T. It is found that $\tau(\theta = 45^\circ)$ decreases slowly as it cools down but drops suddenly around temperature $T = 33$ K. The drop of $\tau(\theta = 45^\circ)$ at $T = 33$ K is due to the presence of vortex torque, which will be addressed in the following discussion.

Figure 1(c) displays the magnetic field H dependence of A measured at 37 K above $T_c = 33$ K. The parameter A exhibits a linear relationship with H^2, suggesting the paramagnetic torque in the normal state, which is derived as below. First, the torque of the material with magnetic moment M under magnetic field H can be written

$$\vec{\tau} = \vec{M} \times \vec{H}. \tag{1}$$

In this equation, $\vec{M}$ can be decomposed into a parallel component $M_\parallel$ and a perpendicular component $M_\perp$ to the sample's ab plane on the basis of parallelogram law. Equation (1) can exchange into

$$\vec{\tau} = (M_\perp H \sin\theta - M_\parallel H \cos\theta)\hat{k}. \tag{2}$$

As we know, under low magnetic field,

$$M_\parallel = \chi_a H_\parallel = \chi_a H \sin\theta$$

and

$$M_\perp = \chi_c H_\perp = \chi_c H \cos\theta,$$

where χ_a and χ_c are the susceptibilities along the a and c axes [16,17]. Finally, we obtain the concrete form of the torque:

$$\tau = \frac{\chi_c - \chi_a}{2} H^2 \sin 2\theta. \tag{3}$$

Since A is proportional to H^2, it can be written as

$$A = C(T)H^2, \tag{4}$$

where C is a fitting parameter with temperature dependence. Combining $\tau = A \sin 2\theta$ and Eq. (4),

$$\tau = A \sin 2\theta = C(T)H^2 \sin 2\theta. \tag{5}$$

From Eqs. (3) and (5), one can easily observe the value of $C = \frac{\chi_c - \chi_a}{2}$. Thus, this linear behavior shows the anisotropy of magnetic moments in two directions of the sample. For FeSCs, the χ_a is bigger than χ_c so the A is negative [18,19], which is different from the heavy fermion superconductor $CeCoIn_5$ [20] and the cuprate superconductor $Bi_2Sr_{2-x}La_xCuO_{6+\delta}$ [21], where χ_c is bigger than χ_a.

Figure 2(a) shows the angular dependent torque measured with increasing angle τ_{inc} and decreasing angle τ_{dec} at the

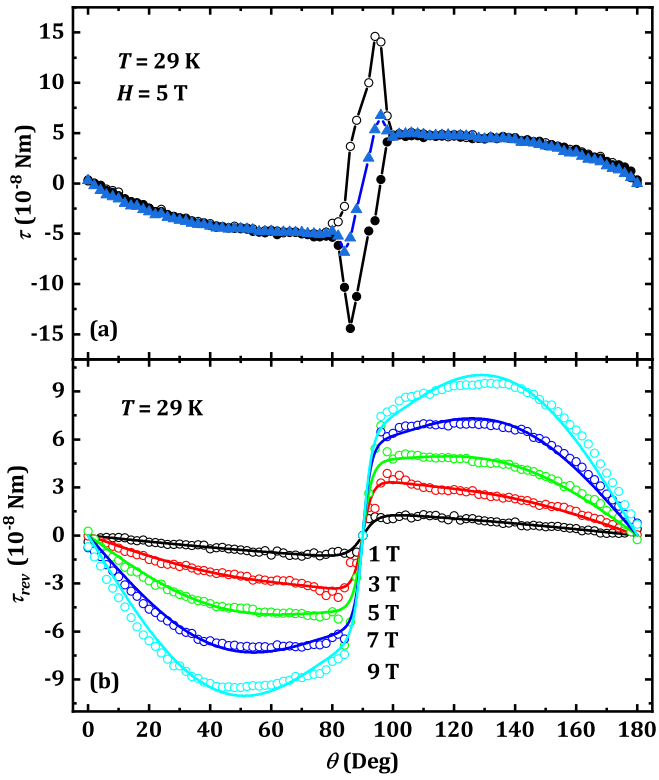

FIG. 2. Torque data measured at $T = 29$ K. (a) The typical angular θ dependent torque data in the mixed sate. The arrows show the torque measured with increasing angle $\tau_{\rm inc}$ and decreasing angle $\tau_{\rm dec}$. The reversible part of the torque data $\tau_{\rm rev}$(blue line) is obtained from the average of $\tau_{\rm inc}$ and $\tau_{\rm dec}$. (b) $\tau_{\rm rev}$ (empty circles) and fitting curves (solid lines) by Eq. (6) for $H = 1$, 3, 5, 7, and 9 T.

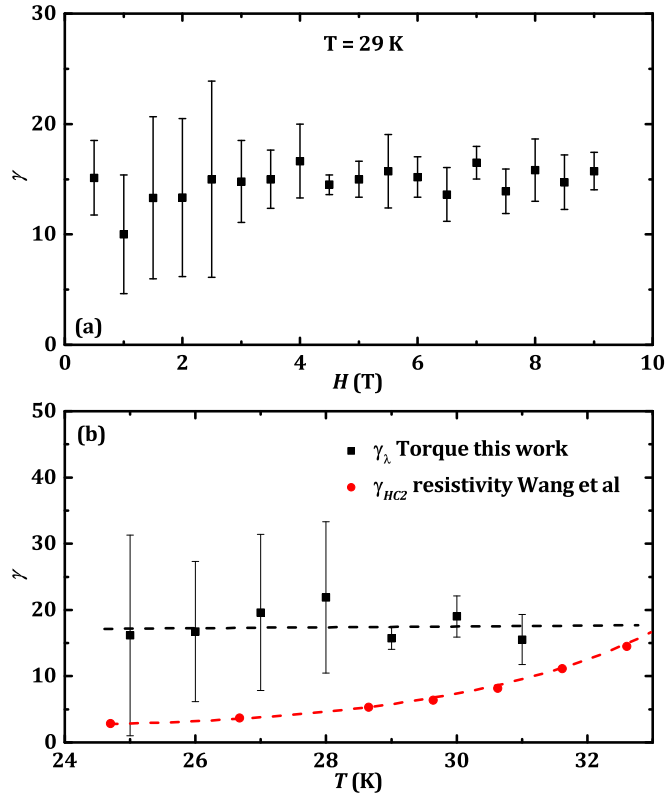

FIG. 3. (a) The magnetic field H dependence of anisotropy parameter γ at temperature $T = 29$ K. (b) Temperature dependence of γ_λ from torque measurements (black points) and γ_{Hc2} obtained from resistivity measurements by Wang *et al.* [23] (red points).

temperature 29 K and magnetic field 5 T in the mixed state. Noted that a large torque hysteresis loop occurs at around 90°. Such a behavior is due to the intrinsic pinning [22] induced by the layered structure of $KCa_2Fe_4As_4F_2$. The reversible component of the torque $\tau_{\rm rev}$ (the blue line) can be obtained by averaging the $\tau_{\rm inc}$ and $\tau_{\rm dec}$ as $\tau_{\rm rev} = (\tau_{\rm inc} + \tau_{\rm dec})/2$.

Figure 2(b) shows $\tau_{\rm rev}$ measured at $T = 29$ K and different applied magnetic fields. Note that the contribution of paramagnetism to the torque ($\sin 2\theta$) in the normal state is too large to be neglected in the mixed state at least near to T_c as shown in Fig. 1(b). Obviously, with the increasing of magnetic field the proportion of $\sin 2\theta$ is more evident. The $\tau_{\rm rev}$ in Fig. 2(b) (open circles) is therefore fitted by the following equation:

$$\tau_{\rm rev}(\theta) = a \sin 2\theta + \frac{\phi_0 HV}{16\pi\mu_0\lambda_{ab}^2}\frac{\gamma^2-1}{\gamma}\frac{\sin 2\theta}{\epsilon(\theta)}\ln\left\{\frac{\gamma\eta H_{c2}^{\|c}}{H\epsilon(\theta)}\right\}. \quad (6)$$

In this equation, $a \sin 2\theta$ is the paramagnetic contribution to $\tau_{\rm rev}$ and the second term is the vortex torque which is given by Kogan's model [13], where V is the volume of the single crystal, λ_{ab} is the penetration depth in the ab plane, $\gamma = \sqrt{m_c/m_a}$ is the anisotropy parameter which is determined according to Ginzburg-Landau theory, $\epsilon(\theta) = \sqrt{\sin^2\theta + \gamma^2\cos^2\theta}$, η is a numerical parameter of the order of unity, and $H_{c2}^{\|c}$ is the upper critical field along the c axis. We define $B = \frac{\phi_0 HV}{16\pi\mu_0\lambda_{ab}^2}$. Note that in Kogan's formula the vortex torque indeed has a negative value at 45°, which thus induces an abrupt decrease at T_c as shown in Fig. 1(c). In order to acquire the anisotropy parameter γ, the torque data can be fitted by Eq. (6) with fitting parameters a, B, and γ. The solid lines in Fig. 2(b) display the fitting results.

Figures 3(a) and 3(b) display the magnetic field dependence of anisotropy parameter γ at 29 K and temperature dependence at 9 T. It shows that γ has a weak temperature and magnetic field dependent behavior. The larger error bars of γ are found at lower temperature and lower field as shown in Figs. 3(a) and 3(b), which is caused by the torque signal that is more scattered at lower magnetic field and more irreversible at lower temperature. It is worth noting that in spite of the same value at around T_c the temperature-dependent γ here from torque measurements is not consistent with the upper critical field anisotropy parameter γ_{Hc2} by resistivity measurements, which decreases with increasing temperature in the superconducting state as shown in Fig. 3(b) [23]. Such a difference was also observed previously and believed to be related to the multiband structure of iron-based superconductors [24]. H_{c2} is usually determined by the superconducting gap. In particular, for an anisotropic multiband superconductor, the mixed two- and three-dimensional superconducting gaps located at different Fermi surfaces govern H_{c2}. On the other hand, the penetration depth is determined by the whole Fermi surface. Thus the multiband structure might cause a different behavior

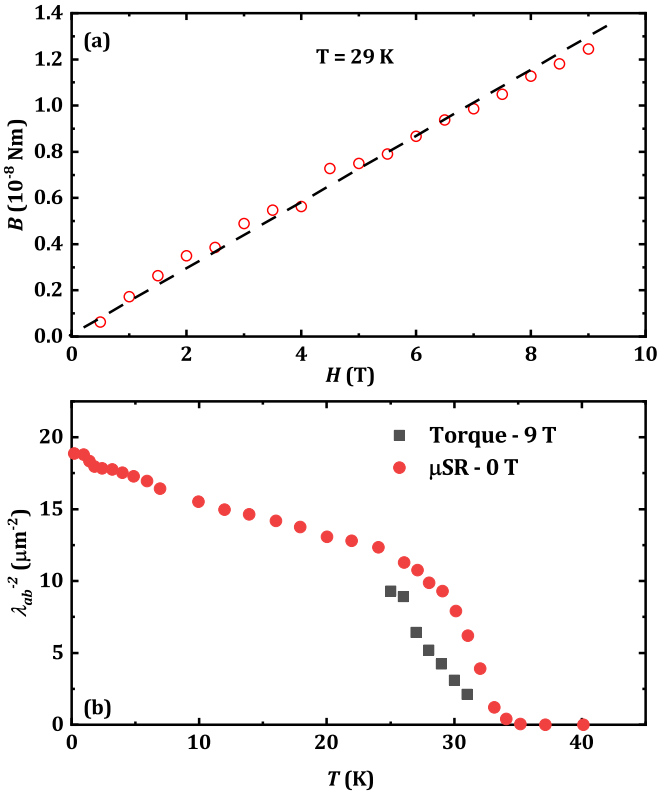

FIG. 4. (a) The magnetic field H dependence of fitting parameter $B = \frac{\phi_0 HV}{16\pi\mu_0\lambda_{ab}^2}$ at temperature $T = 29$ K. (b) The temperature T dependence of penetration depth λ_{ab}^{-2} (black points) under magnetic field $H = 9$ T and data of polycrystalline $KCa_2Fe_4As_4F_2$ measured by μSR at zero field (red points).

of γ_λ and γ_{Hc2} [25]. It is found that, at $T = 25$ K ($\approx 0.76\ T_c$), $\gamma = 16.2$, which is close to the result of $CaFe_{0.88}Co_{0.12}AsF$, $\gamma \approx 15$ at $T \approx 0.76\ T_c$) [19]. However, comparing with the 11 and 122 families [26], where γ is around 3, the 12442 family is more anisotropic in the superconducting state. This may suggest that the electronic coupling between layers in the 12442 family is weaker than in the 11 and 122 families in the superconducting state.

Figure 4(a) shows the curve of the magnetic field dependence of the parameter $B = \frac{\phi_0 HV}{16\pi\mu_0\lambda_{ab}^2}$. It is found that B displays a linear H dependent behavior. Thus, the in-plane penetration depth λ_{ab} is a field H independent constant. This behavior is similar to the result of $CeCoIn_5$, the B of which shows linear behavior at low field [20]. The black points in Fig. 4(b) show temperature dependence of λ_{ab}^{-2} with magnetic field $H = 9$ T. The red lines show the results of μSR measured on a polycrystalline sample at $H = 0$ T [27]. It is found that the black points are a little smaller than the red points. The shift is due to the different applied magnetic fields for the torque and μSR measurements on λ_{ab}^{-2}, which is usually suppressed by the magnetic field [28]. Thus these two results are consistent.

IV. CONCLUSION

In summary, detailed angular dependent torque measurements were performed on $KCa_2Fe_4As_4F_2$. The paramagnetism is found to govern the torque signal in the normal state. We get the anisotropy parameter γ at different temperatures and magnetic fields in the mixed state through fitting the data with Kogan's model. The value of γ is similar to the 1111 family but larger than 11 and 122 families. The penetration depth of $KCa_2Fe_4As_4F_2$ at temperatures below T_c is comparable with the results of μSR measured on polycrystalline samples.

ACKNOWLEDGMENTS

The authors acknowledge the support of National Natural Science Foundation of China Grant No. 11574338, National Natural Science Foundation of China - China Academy of Engineering Physics NSAF Joint Fund Grant No. U1530402, and Chinese Academy of Sciences State Key Laboratory of Functional Materials for Informatics.

[1] Z. Wang, C. He, S. Wu, Z. Tang, Y. Liu, A. Ablimit, C. Feng, and G. Cao, J. Am. Chem. Soc. **138**, 7856 (2016).
[2] Z. Wang, C. He, Z. Tang, S. Wu, and G. Cao, Sci. Chin. Mater. **60**, 83 (2017).
[3] Z. C. Wang, C. Y. He, S. Q. Wu, Z. T. Tang, Y. Liu, A. Ablimit, Q. Tao, C. M. Feng, Z. A. Xu, and G. H. Cao, J. Phys. Condens. Matter **29**, 11LT01 (2017).
[4] Z. Wang, C. He, S. Wu, Z. Tang, Y. Liu, and G. Cao, Chem. Mater. **29**, 1805 (2017).
[5] S. Q. Wu, Z. C. Wang, C. Y. He, Z. T. Tang, Y. Liu, and G. H. Cao, Phys. Rev. Mater. **1**, 044804 (2017).
[6] T. Wang, J. Chu, H. Jin, J. Feng, L. Wang, Y. Song, C. Zhang, X. Xu, W. Li, Z. Li, T. Hu, D. Jiang, W. Peng, X. Liu, and G. Mu, J. Phys. Chem. C **123**, 13925 (2019).
[7] B. Wang, Z. C. Wang, K. Ishigaki, K. Matsubayashi, T. Eto, J. Sun, J. G. Cheng, G. H. Cao, and Y. Uwatoko, Phys. Rev. B **99**, 014501 (2019).
[8] G. Wang, Z. Wang, and X. Shi, EPL **116**, 37003 (2016).
[9] Z. C. Wang, Y. Liu, S. Q. Wu, Y. T. Shao, Z. Ren, and G. H. Cao, Phys. Rev. B **99**, 144501 (2019).
[10] J. Ishida, S. Iimura, and H. Hosono, Phys. Rev. B **96**, 174522 (2017).
[11] Z. Wang, G. Wang, and X. Tian, J. Alloys Compd. **708**, 392 (2017).
[12] M. Tinkham, *Introduction to Superconductivity* (Courier Corporation. Mineola, New York, 2004).
[13] V. G. Kogan, Phys. Rev. B **38**, 7049 (1988).
[14] K. Hashimoto, Y. Mizukami, R. Katsumata, H. Shishido, M. Yamashita, H. Ikeda, Y. Matsuda, J. A. Schlueter, J. D. Fletcher, and A. Carrington, Proc. Natl. Acad. Sci. USA **110**, 3293 (2013).
[15] Z. Shermadini, A. Krzton-Maziopa, M. Bendele, R. Khasanov, H. Luetkens, K. Conder, E. Pomjakushina, S. Weyeneth, V. Pomjakushin, O. Bossen *et al.*, Phys. Rev. Lett. **106**, 117602 (2011).

[16] S. Kasahara, H. J. Shi, K. Hashimoto, S. Tonegawa, Y. Mizukami, T. Shibauchi, K. Sugimoto, T. Fukuda, T. Terashima, and A. H. Nevidomskyy, Nature (London) **486**, 382 (2012).

[17] R. Okazaki, T. Shibauchi, H. J. Shi, Y. Haga, T. D. Matsuda, E. Yamamoto, Y. Onuki, H. Ikeda, and Y. Matsuda, Science **331**, 439 (2011).

[18] A. S. Sefat, R. Jin, M. A. McGuire, B. C. Sales, D. J. Singh, and D. Mandrus, Phys. Rev. Lett. **101**, 117004 (2008).

[19] H. Xiao, B. Gao, Y. H, X. J. Li, G. Mu, and T. Hu, J. Phys. Condens. Matter **28**, 325701 (2016).

[20] H. Xiao, T. Hu, C. C. Almasan, T. A. Sayles, and M. B. Maple, Phys. Rev. B **73**, 184511 (2006).

[21] H. Xiao, Phys. Rev. B **90**, 214511 (2014).

[22] T. Ishida, K. Okuda, H. Asaoka, Y. Kazumata, K. Noda, and H. Takei, Phys. Rev. B **56**, 11897 (1997).

[23] T. Wang, C. Zhang, L. Xu, J. Wang, S. Jiang, Z. Zhu, Z. Wang, J. Chu, J. Feng, L. Wang, W. Li, T. Hu, X. Liu, and G. Mu, Sci. Chin. Phys. Mech. (to be published).

[24] M. Bendele, S. Weyeneth, R. Puzniak, A. Maisuradze, E. Pomjakushina, K. Conder, V. Pomjakushin, H. Luetkens, S. Katrych, A. Wisniewski, R. Khasanov, and H. Keller, Phys. Rev. B **81**, 224520 (2010).

[25] V. Kogan, Phys. Rev. Lett. **89**, 237005 (2002).

[26] R. Khasanov and Z. Guguchia, Supercond. Sci. Technol. **28**, 034003 (2015).

[27] A. Bhattacharyya, D. Adroja, M. Smidman, and V. Anand, Sci. Chin. Phys. Mech. **61**, 127402 (2018).

[28] R. Khasanov, T. Kondo, S. Strässle, D. O. G. Heron, A. Kaminski, H. Keller, S. L. Lee, and T. Takeuchi, Phys. Rev. B **79**, 180507(R) (2009).